PHYSICS AND CHEMISTRY OF SOLID STATE
V. 25, No. 4 (2024) pp. 773-781
Section: Physics

DOI: 10.15330/pcss.25.4.773-781

Vasyl Stefanyk Precarpathian National University

ФІЗИКА І ХІМІЯ ТВЕРДОГО ТІЛА
Т. 25, № 4 (2024) С. 773-781
Фізико-математичні науки

PACS: 02.30.Nw, 61.05.J-, 62.20.-x, 62.20.F-, 68.35.Gy, 81.05.ug

ISSN 1729-4428 (Print)
ISSN 2309-8589 (Online)

M. Fodchuk[1*], S.V. Balovsyak[1], M.S. Solodkyi[1], M.D. Borcha[1], D.-I. Băilă[2], R. Labudzki[3], M. Bonilla[4]

Spatial distributions of local strains in synthesized diamond crystals from the normalized parameters of Kikuchi patterns

[1]*Yuriy Fedkovych Chernivtsi National University, Chernivtsi, Ukraine, i.fodchuk@chnu.edu.ua*
[2]*National University of Science and Technology Politehnica Bucharest, Bucharest, Romania*
[3]*Poznan University of Technology, Poznań, Poland*
[4]*Edibon International S.A., Mostoles, Spain*

This paper presents an improved approach to the calculation and analysis of spatial distributions of local strains in synthesized diamond crystals obtained from the normalized parameters of Kikuchi patterns. This approach consists in the study of Kikuchi patterns using normalized Kikuchi band profiles and the normalized characteristics of the energy Fourier spectrum of the diffraction patterns. The spatial strain distribution for 6 samples of polycrystalline artificial diamond was studied. A cluster analysis of the investigated crystal samples was carried out, which made it possible to establish relationships between the conditions of diamond crystal growth and their strain distributions.

Keywords: synthesized diamonds, electron backscatter diffraction, Kikuchi pattern, strain distribution, Fourier transform, energy Fourier spectrum, cluster analysis.

Received 23 June 2024; Accepted 12 November 2024.

Introduction

Synthesized diamond has a polycrystalline structure, and its crystallites are heterogeneous and contain entire complexes of defects [1-7]. This causes significant restrictions on technological innovation in diamond application and has a significant impact on the mechanical, electrical and optical properties of these crystals [8-11]. Important characteristics of diamond crystals are structural strains that arise as a result of non-uniform distributions of deformations ε. They are determining through a changes in the interplanar distances $\Delta d/d$.

Among the methods for determining crystal deformations, methods based on the analysis of electron backscattering diffraction images (Kikuchi patterns) are particularly promising due to their high locality and non-destructive nature of the research [12-19]. Based on the study of the shape of the profiles of intensity distribution across the single bands (further in the text – band profiles) and the energy Fourier spectrum of Kikuchi patterns from each crystallite, it became possible to determine local deformations in individual regions of crystals. The approaches to analyzing Kikuchi band profiles given in [2, 5, 12, 15, 20] provide for a comparison of the regions of the band profiles obtained from different regions of a single crystallite with the region of the profile obtained from a reference crystal or unstrained region of the researched crystal. From the analysis of the energy spectrum of intensity distributions in the approaches [5, 21-24], one of the crystallite is used as a reference, with respect to which deformations in others are determined. However, in many cases, the choice of an unstrained crystallite is difficult or impossible. This significantly complicates estimating deformations and the comparison their values between different crystals or crystallites.

The results obtained in [2, 5, 20] demonstrate the limitations of this approach. Therefore, a new approach is required for a detailed study of properties in local regions (crystallites) and further in different crystallographic

directions.

This paper proposes a modified approach for determining local deformations in individual regions (crystallites) of artificial diamond crystals. This approach consists in the study of Kikuchi patterns without using a reference image that is using normalized Kikuchi band profiles and the normalized characteristics of the energy Fourier spectrum of the diffraction patterns. This opens up the possibility of analysis and comparison of local strain distributions for different polycrystalline systems, allows studying the influence of growing conditions on the structural homogeneity and stress (strain values) of the samples.

I. Experimental part

A series of artificial diamond samples (D1-D6) synthesized under different conditions (see Table 1) are studied [15, 20, 25-27]. Research was carried out using a Zeiss EVO-50 scanning electron microscope using a CCD detector. The incidence angle of the electron beam (diameter ~ 40 nm) on the crystal surface was 70°.

Cathodoluminescent topograms of diamond polycrystalline surfaces in the case of artificially grown samples are shown on Fig.1. Markers indicate the positions of the regions for which Kikuchi patterns were obtained (Fig. 2). These images were presented in digital form f in the $M \times N$ pixel format.

Table 1.

Synthesis parameters of the studied artificial diamond crystals

№	Sample name	Temperature T, °K	Pressure P, GPa	System	Substrate
1	D1	1650	4.5-6	Fe-Co-C	Ni-Mn-C
2	D2	1800	7	Mg-C + B	Ni-Mn-C
3	D3	1700	6	Fe-Al-C	Ni-Mn-C
4	D4	1650	4.5-6	Fe-Co-C	Ni-Mn-C
5	D5	1600	5.7	Fe-Co-C	Ni-Mn-C
6	D6	1650	4.5-6	Fe-Co-C	Ni-Mn-C

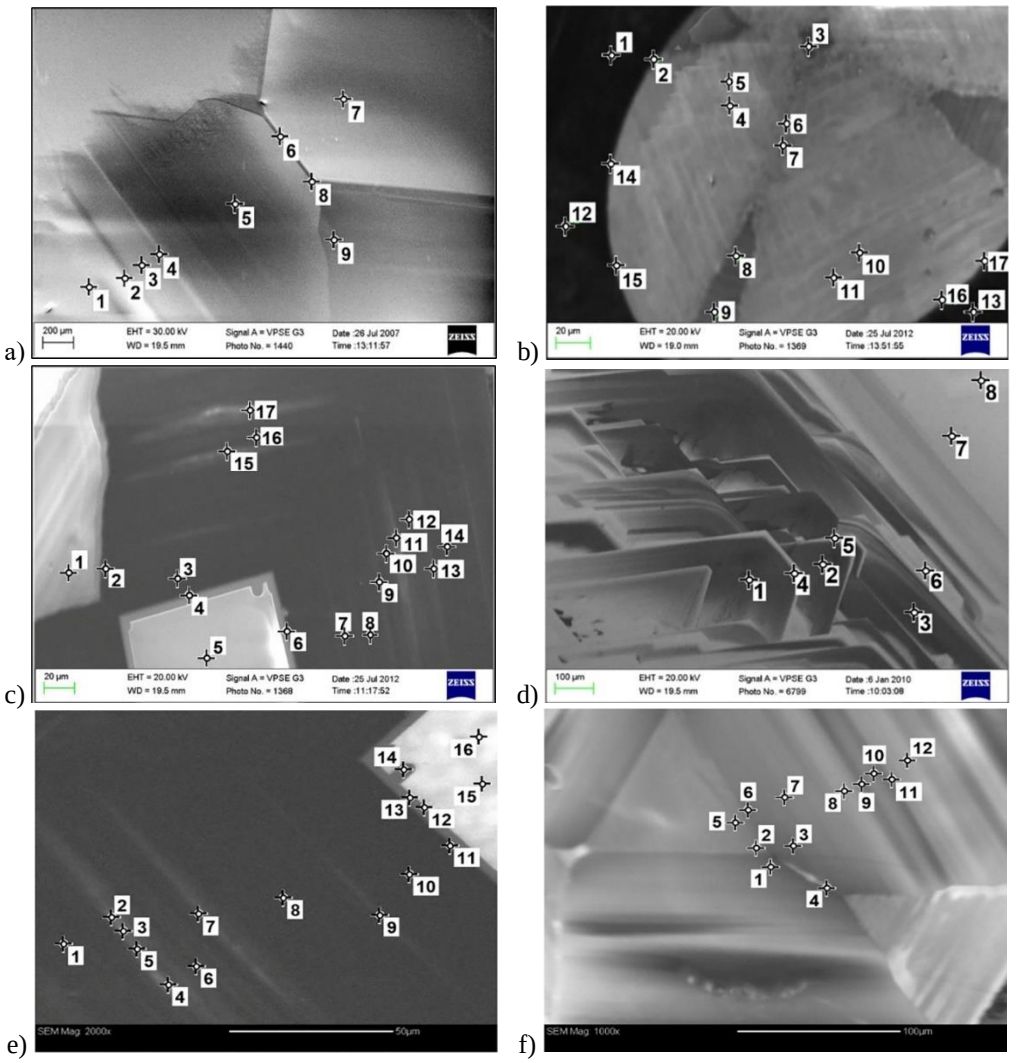

Fig. 1. Fragments of cathodoluminescent images of artificial diamond crystal surfaces: a) crystal D1, fragment size is 3.0×2.0 mm; b) D2 (280×180 μm); c) D3 (300×225 μm); d) D4 (1.2×0.8 mm); e) D5 (140×115 μm); f) D6 (280×200 μm).

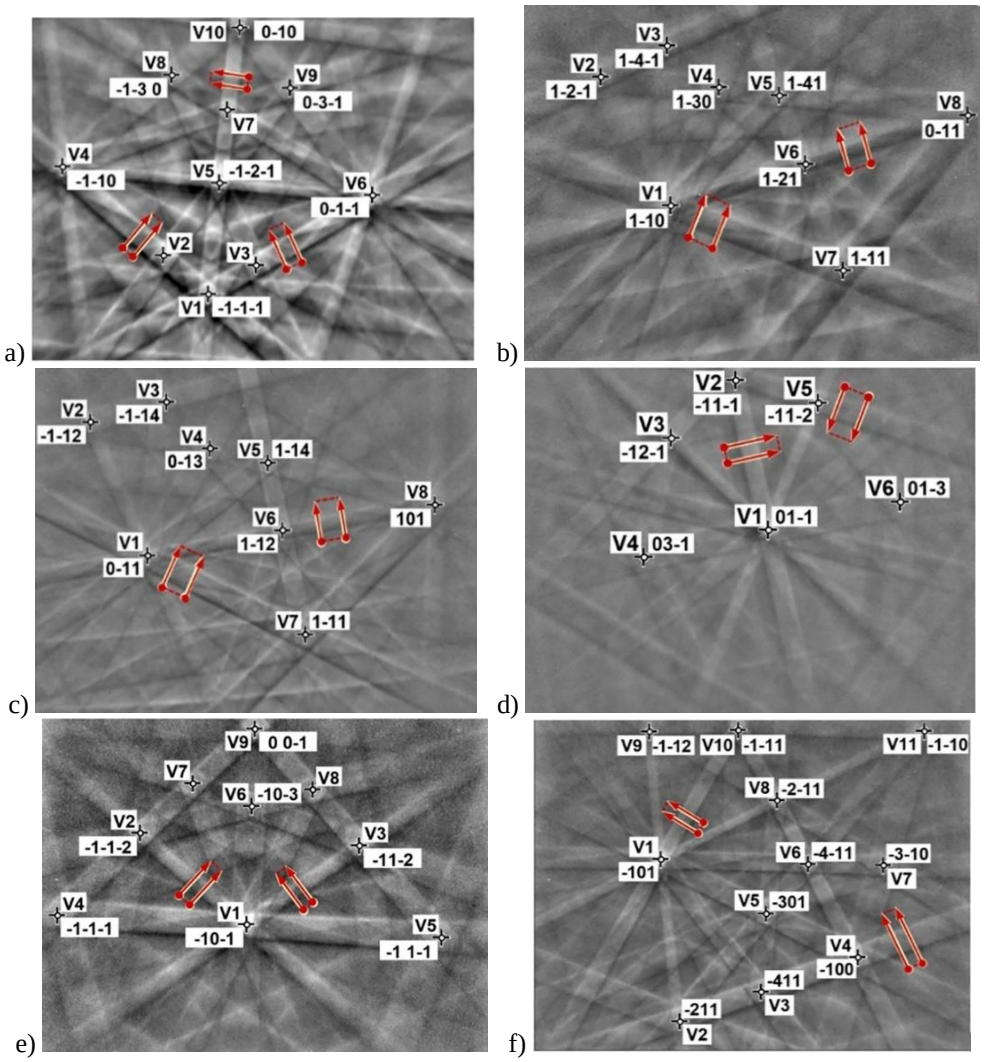

Fig. 2. Experimental Kikuchi patterns obtained from (Fig. 1): a) region No. 1 of crystal D1; b) region No. 1 of crystal D2; c) region No. 1 of crystal D3; d) region No. 8 of crystal D4; d) region No. 1 of crystal D5; e) region No. 1 of crystal D6. The "+" markers indicate the nodes V of intersections of Kikuchi bands which correspond to direction indices (zone axes) [u v w]; the arrows show the fragments of the bands for which the profiles were calculated.

The intensity distribution across the Kikuchi bands (Fig. 2) in the crystalline regions designated by numbers (Fig. 1) depends not only on the reflecting crystallographic plane, but also on the magnitude of the crystal lattice strains. Our goal is to obtain a comparative characteristic of the deformation distributions for a given series of crystals through the corresponding analysis of the intensity distribution profiles across the Kikuchi band [12, 20, 24].

The intensity distribution over the entire Kikuchi pattern depends not only on the characteristics of the studied samples, but also on the experimental conditions (instrumental factors). This significantly complicates the analysis of experimental images. Intensity distortions of the Kikuchi patterns caused by noise in the photosensitive matrix, as well as changes in the average brightness and contrast of the patterns. At the same time, the impulse and Gaussian noises are dominate on the experimental images of Kikuchi bands (Fig. 2). Geometric distortions of the patterns (shift of the band images in height and width, their stretching, compression and rotation) caused by changing the incidence angle of electrons on the sample, the distance from the sample to the detector, etc. To reduce the influence of instrumental factors, software was developed (using the MATLAB) for sequential digital processing of Kikuchi bands images [28, 29]. To compensate geometric distortions using genetic and gradient algorithms [21, 29], all images of one series (obtained from one crystal) were transformed into one scale by combining them with a reference image (obtained from region No. 1 of crystal D1).

II. General provisions

To determine the magnitudes and distributions of deformations specific techniques were used in [15, 20, 25, 26, 30-33]. In these techniques the degree of blurring of the diffraction bands and their intersections caused by deformations is quantitatively described through the intensity distribution on the Kikuchi bands [30]. In this paper we propose modification of approach, developed in [31-33] where the methods of the energy Fourier spectrum and the discrete two-dimensional Fourier transform used.

2.1. Determining the magnitude of deformations from the analysis of normalized profiles of the intensity distribution of Kikuchi bands

Average profiles of Kikuchi bands on digital images *f* (Fig. 3) are calculated as the average value of a series of profiles for a segment of a band (Fig. 2) using software created in the MATLAB environment [28].

By averaging the intensity of the profiles *I(r)* (where *r* is the length of the profile), the signal-to-noise ratio for the resulting profile is increased and its shape is more accurately reproduced. Averaged profiles were calculated for the most intense bands, for example, in the Kikuchi pattern (Fig. 2a), as well as profiles for bands between nodes *V2V4*, *V3V6*, and *V1V5*. The intensity of the calculated profiles of the Kikuchi bands was normalized in the given range (0, 1), due to which the influence of instrumental factors on the shape of the profile was reduced.

Non-uniform distributions of deformations in crystals lead to distortions of the distribution of the intensities of the Kikuchi bands, therefore the local deformation ε_{PV} of the crystal for a certain crystallographic plane can be calculated based on the area under the intensity profile *I(r)* of the Kikuchi band according to the relation [12]:

$$\varepsilon_{PV} = k_d \, ln\left(\frac{S_P}{S_{P0}}\right), \quad (1)$$

where $k_d = 3.76 \cdot 10^{-3}$; S_P is the normalized area under the Kikuchi band intensity profile for region with deformation, $S_{P0} = 0.45$ is the normalized area for region without deformation.

Due to the normalization of areas S_P and S_{P0} under Kikuchi band intensity profile (dividing the sum of the values of the profile *I(r)* by its width W_r) provides the dependence of S_P and S_{P0} only of the profile shape, and also the possibility of analyzing profiles of different widths for Kikuchi patterns, obtained for region of different crystals.

2.2. Determination of local strains by analyzing the energy spectrum normalized parameters

Crystal deformations affect the spatial distribution of the intensity of Kikuchi patterns, and, accordingly, their Fourier energy spectra. This allows to describe the relationship between crystal deformations ε_T and the characteristics of the spectra of Kikuchi patterns, for example, with their average spatial radial frequency $\overline{v}_R$ or with the average spatial radial period $\overline{T}_R = \frac{1}{\overline{v}_R}$ [34].

The average spatial radial frequency $\overline{v}_R$ is calculated based on the radial distribution of P_R in the frequency range from $v_{min} = 1/T_r^{max}$ to $v_{max} = 1/T_r^{min}$ [34]:

$$\overline{v}_R = \frac{\sum_{d=d_1}^{d=d_2} P_R(d) v_r(d)}{\sum_{d=d_1}^{d=d_2} P_R(d)}, \quad (2)$$

where $d_1 = [N_{min} T_r^{max}]$, $d_2 = [N_{min} T_r^{min}]$, $N_{\min} = \min(M, N)$ – is the minimum image size *f*, the value of periods $T_r^{min} = 5$ pixels and $T_r^{max} = 75$ pixels, respectively.

Quantitatively, the relationship between the crystal strains ε_T and the averaged spatial radial frequencies $\overline{v}_R$ (and associated periods $\overline{T}_R = \frac{1}{\overline{v}_R}$) of the spectra of Kikuchi pattern is described in the form of an empirical relationship:

$$\varepsilon_T = k_T \cdot ln\left(\frac{\overline{v}_{N0}}{\overline{v}_N}\right), \quad (3)$$

where $k_T = 2.16 \times 10^{-3}$ (chosen to match the average strain values ε_P and ε_T taking into account the data of [12]); $\overline{v}_{N0} = 0.075\ pixels^{-1}$ normalized average spatial radial frequency for the region without deformation (it is chosen as the maximum value of the normalized frequency for Kikuchi patterns); $\overline{v}_N$ – normalized average spatial radial frequency, which is calculated with the equation:

$$\overline{v}_N = \frac{\overline{v}_R - v_{min}}{v_{max} - v_{min}}, \quad (4)$$

Frequency $\overline{v}_N$ normalization ensures its independence from instrumental factors, in particular, from the influence of noise and the average background of the image. Using the same value $\overline{v}_{N0}$ for all Kikuchi patterns allows to calculate and compare strain values for different regions of diamond crystals.

III. Results

The obtained strain values ε_{PV} for local regions *s* of diamond crystals differ depending on the reflecting crystallographic planes, which indicates a certain anisotropy in the distributions of deformations [20, 25].

For each investigated region of diamond crystals (Fig. 1), the average values of ε_P strains (Fig. 3) were calculated based on the values of ε_{PV} strains obtained by analyzing the profiles of Kikuchi bands for different crystallographic planes.

The calculation of the strains ε_T of artificial diamond crystals based on the energy spectra of Kikuchi patterns was performed using the developed software in the MATLAB environment.

The satisfactory agreement between the values of ε_P and ε_T (Fig. 3) testifies to the correctness of the proposed method of determining strains based on the profiles of Kikuchi bands and the energy spectra of Kikuchi patterns.

Based on the obtained values of deformations ε by their approximation, the spatial distribution of deformations was calculated in the form of level lines (Fig. 4) and in the form of a three-dimensional surface for local regions of crystals (Fig. 5).

The strain distributions calculated from diamond Kikuchi patterns qualitatively agrees with the data obtained from cathodoluminescent images on Fig. 1. In particular, for crystal D1 (Fig. 1a), the strain values in regions 1, 2, 3, 4, 5 gradually decrease; at the same time, the strain values in region 5, which is in the center of a large homogeneous part, are minimal. Corresponding agreements between strain values observed for regions 6 and 8, 7 and 9.

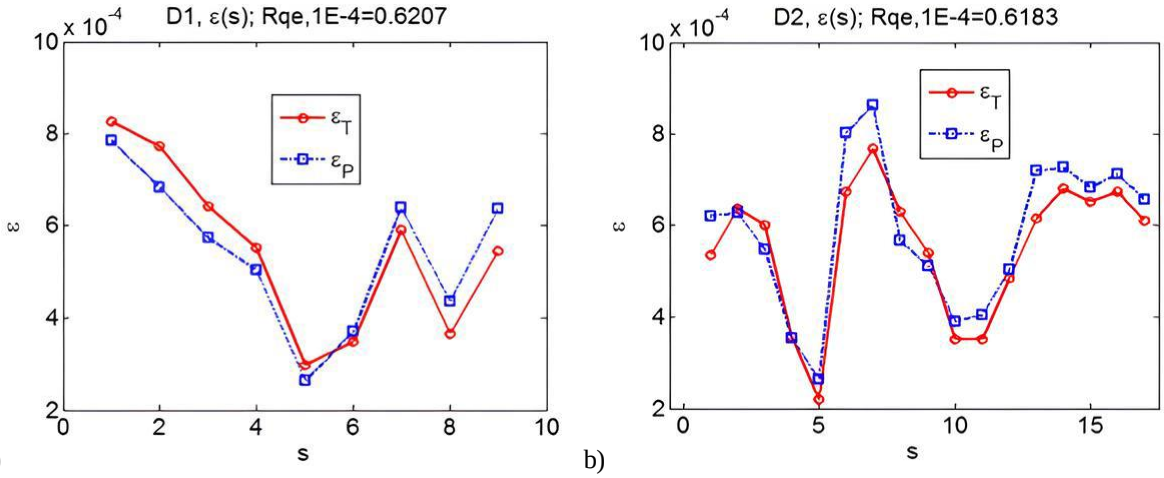

Fig. 3. Values of average strains ε_P calculated on the basis of the Kikuchi band profiles, and strains ε_T on the basis of the energy spectrum of the Kikuchi pattern for local region *s* of crystals: a) crystal D1 (Fig. 1a); b) crystal D2 (Fig. 1b); c) crystal D3 (Fig. 1c); *Rqe* is the root-mean-square difference between the values of ε_P and ε_T.

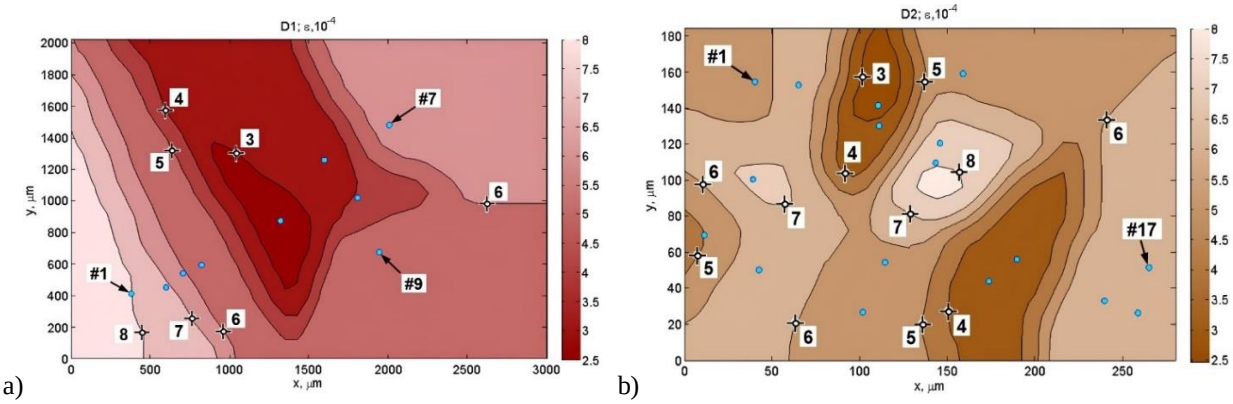

Fig. 4. Map of the spatial strain distribution ε in the form of level lines, marked with crosses, for local regions of artificial diamond crystals: a) crystal D1 (Fig. 1a); b) crystal D2 (Fig. 1b); the position of the regions for which the image of Kikuchi bands was obtained is shown by markers #.

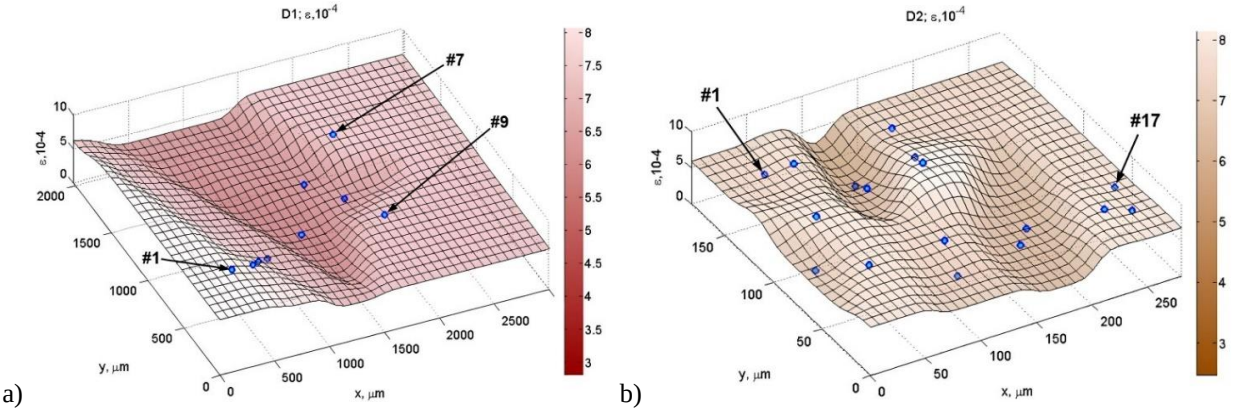

Fig. 5. Map of spatial strain distributions in the form of a three-dimensional surface for local regions of artificial diamond crystals: a) crystal D1 (Fig. 1a); b) crystal D2 (Fig. 1b); the position of regions for which the image of Kikuchi bands was obtained is shown by markers.

For crystal D2 (Fig. 1b), the strain values in region 1, 12, 13, which are outside the boundaries of the bright disk, are similar. The strains in region 2, 14, 15, 16, 17, which are found on the perimeter of the bright disc, are also close. The smallest deformations were obtained in regions 4 and 5, as well as in regions 10 and 11, which are located in homogeneous parts of the crystal. Relatively large strains observed in regions 3, 6, 7, 8, 9, which are close to the interface between two crystallites of the crystal.

For the purpose of quantitative analysis of artificial diamond crystal strains, the following parameters were determined (Table 2) [20, 25, 26, 35, 36]:

- minimum ε_{min} and maximum ε_{max} values of strains ε;
- the range D_ε of strain values, which describes the maximum change in deformation state (defined as the

Table 2.

Strain parameters for the studied diamond crystals

№	Name	ε_{min}, 10^{-4}	ε_{max}, 10^{-4}	D_ε, 10^{-4}	M_ε, 10^{-4}	σ_ε, 10^{-4}	$A_{S\varepsilon}$	K_ε	$\sigma_\varepsilon / M_\varepsilon$
1	D1	2.8	8.1	5.2	5.4	1.6	-0.11	1.96	0.29
2	D2	2.4	8.3	5.7	5.7	1.5	-0.56	2.46	0.26
3	D3	1.4	4.2	2.8	2.8	0.8	0.23	2.09	0.29
4	D4	2.9	8.8	5.9	5.6	1.7	0.36	2.48	0.30
5	D5	2.4	5.2	2.7	3.5	0.8	0.86	2.60	0.24
6	D6	5.3	7.4	2.1	6.6	0.6	-0.54	2.08	0.10

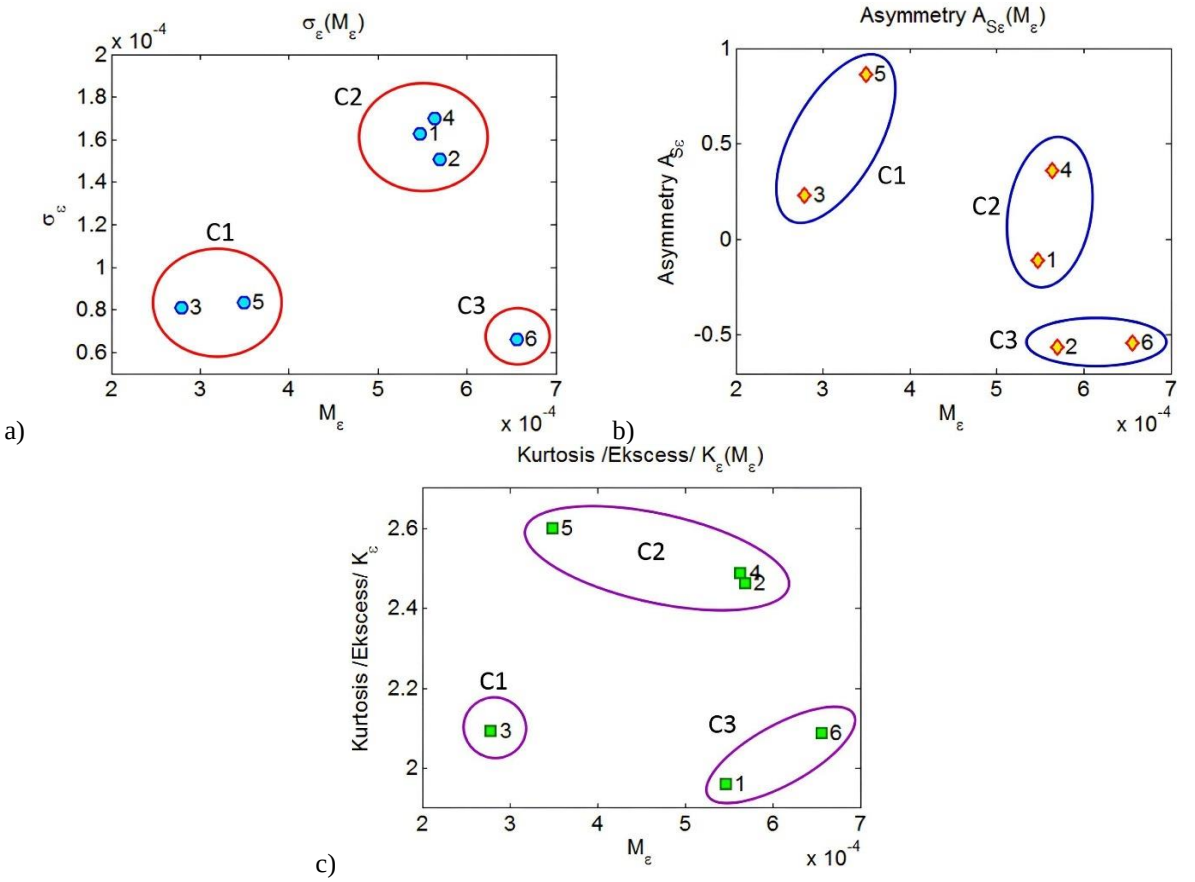

Fig. 6. Clustering of the studied diamond crystals based on their strain parameters ε: a) coordinate system (σ_ε, M_ε); b) coordinate system ($A_{S\varepsilon}$, M_ε); c) coordinate system (K_ε, M_ε); crystal numbers D1-D6 are indicated by numbers.

difference between the maximum and minimum values of ε);

- the average arithmetic values M_ε and the standard deviation σ_ε of the strains ε;
- asymmetry $A_{S\varepsilon}$, which determines the symmetry of the strain values ε relative to the average value of M_ε;
- kurtosis K_ε, which describes the nature of the deviation of the strain values ε from the average value M_ε.

For a deeper analysis of the obtained data (Table 2), clustering of the studied diamond crystals in the space of their strain parameters was carried out (Fig. 6). Clustering was performed by the k-means method using the Euclidean distance between points using the developed software.

When clustering in the coordinate system (σ_ε, M_ε) (Fig. 6a), crystals D3 and D5 belong to class C1, which are characterized by relatively low average strain values M_ε and their insignificant mean of standard deviation σ_ε. This can be explained by the synthesis conditions of crystals D3 and D5: growing by the method of temperature gradient on the "seed" with a growth rate of ≈ 2.7 mg/hour, which contributes to the minimal inclusion of the catalyst during growth. Class C2 includes crystals D1, D2, and D4, which are characterized by high values of M_ε and σ_ε; this can be explained by the uneven distribution of nitrogen and boron impurities during crystal growth. The D6 crystal belongs to the C3 class, which is characterized by a high value of M_ε and a low value of σ_ε; at the same time, significant average strain values can be explained by the uneven distribution of impurities during growth, as well as by the complex topography of the crystal.

Conclusions

1. The spatial distribution of deformations was determined for 6 samples of polycrystalline artificial diamond. Satisfactory agreement between the strain values obtained by proposed approach and by approaches of other authors indicates the correctness of the first of

them for determining strains from the analysis of Kikuchi band profiles using energy spectra of Kikuchi patterns.

2. Approaches for characterization of the structure and study of the deformation state in artificial diamond crystals based on multi-beam diffraction of backscattered electrons are presented and can provide important information for controlling the technological process and predicting electrical and optical properties during the study of crystals.

3. Clustering in the space of strain parameters was carried out for a series of diamond crystals with the k-means method using the Euclidean distance between points on the dependence of the standard strain deviation σ_ε on the average arithmetic values M_ε of the strains. This helped us to establish a relationship between crystal growth conditions and their strain characteristics. So, D3 and D5 crystals belong to class C1, which are characterized by relatively low average values of deformations M_ε and mean of standard deviation σ_ε. For these samples, combination of growth system and temperature-pressure mode of growth contributes to the formation of more homogeneous structure. D1, D2 and D4 crystals belong to class C2 with high values of M_ε and σ_ε, which is explained by the uneven distribution of nitrogen and boron impurities during growth. Crystal D6 (class C3) has a high value of M_ε and low σ_ε, which is explained by the non-ideal topography of the crystal and the uneven distribution of impurities.

Acknowledgments

This work was funded by the Erasmus+ Programme Key Action 2 Cooperation Partnerships for Higher Education (KA220-HED), project number 2023-1-RO01-KA220-HED-000155412, with the title "European Network for Additive Manufacturing in Industrial Design for Ukrainian Context" – AMAZE, contract nb. 3512/27.10.2023.

Fodchuk I.M. – Doctor of Physics and Mathematics Sciences, Professor;
Balovsyak S.V. – Doctor of Technical Sciences, Associate Professor;
Solodkyi M.S. – Candidate of Physics and Mathematics Sciences, Assistant Lecturer;
Borcha M.D. – Doctor of Physics and Mathematics Sciences, Associate Professor;
Băilă D.-I. – Doctor of Engineering, Professor;
Labudzki R. – Doctor of Engineering, Senior Lecturer;
Bonilla M. – Vice President of Edibon International S.A.

[1] L.A. Roshan, A.K. Ramdas, *Physical Properties of Diamond and Sapphire* (CRC Press, Boca Raton, 2019); https://doi.org/10.1201/9780429283260.
[2] N.V. Novikov, T.A. Nachalna, S.A. Ivakhnenko, O.A. Zanevsky, I.S. Belousov, V.G. Malogolovets, G.A. Podzyarei, L.A. Romanko, *Properties of semiconducting diamonds grown by the temperature-gradient method*, Diamond and Related Materials, 12(10-11), 1990 (2003); https://doi.org/10.1016/S0925-9635(03)00317-0.
[3] V.V. Lysakovskyi, S.O. Ivakhnenko, T.V. Kovalenko, V.M. Kvasnytsya, A.V. Burchenia, *Morphology of diamond single crystals grown in the Fe-Co-Ti(Zr)-C system*, Journal of Crystal Growth, 578, 126422 (2022); https://doi.org/10.1016/j.jcrysgro.2021.126422.
[4] Y. Wang, Z. Wang, Z. Lu, Z. Cai, S. Fang, H. Zhao, H. Jia, H. Ma, L. Chen X. Jia, *The characteristics of Ib diamond crystals synthesized in a Fe–Ni–C system with different SiC contents*, CrystEngComm, 23(35), 6070 (2021); https://doi.org/10.1039/D1CE00590A.
[5] I.M. Fodchuk, V.M. Tkach, V.G. Ralchenko, A.P. Bolshakov, E.E. Ashkinazi, I.I. Vlasov, Y.D. Garabazhiv, S.V. Balovsyak, S.V. Tkach, O.M. Kutsay, *Distribution in angular mismatch between crystallites in diamond films*, Diamond and Related Materials. 19(5-6), 409 (2010); https://doi.org/10.1016/j.diamond.2010.01.020.
[6] J. E. Field, *The mechanical and strength properties of diamond*, Reports on Progress in Physics, 75(12), 126505 (2012); https://doi.org/10.1088/0034-4885/75/12/126505.
[7] S. Kaboli, P. C. Burnley, *Direct observations of crystal defects in polycrystalline diamond*, Materials Characterization, 142, 154 (2018); https://doi.org/10.1016/j.matchar.2018.05.036.
[8] S. Koizumi, H. Umezawa, J. Pernot, M. Suzuki, *Power Electronics Device Application of Diamond Semiconductors* (Woodhead Publishing, Duxford, 2018);
[9] F. Zhao, Y. He, B. Huang, T. Zhang, H. Zhu, *A Review of Diamond Materials and Applications in Power Semiconductor Devices*, Materials, 17(4), 3437 (2024); https://doi.org/10.3390/ma17143437.
[10] P. Hazdra, A. Laposa, Z. Šobáň, J. Kroutil, N. Lambert, V. Povolný, A. Taylor, V. Mortet, *Pseudo-Vertical Schottky Diode with Ruthenium Contacts on (113) Boron-Doped Homoepitaxial Diamond Layers*, Physica Status Solidi A, 220(23), 2300508 (2023); https://doi.org/10.1002/pssa.202300508.
[11] Y. Seki, M. Yoshihara, S.-W. Kim, K. Koyama, Y. Hoshino, *Light B Doping by Ion Implantation into High-Purity Heteroepitaxial Diamond*, Physica Status Solidi A, 221(18), 2400159 (2024); https://doi.org/10.1002/pssa.202400159.
[12] Y. Sasaki, M. Igushi, M. Hino, *Measuring strains for hematite phase in sinter ore by electron backscattering diffraction method*, Key Engineering Materials, 326-328, 237 (2006); https://doi.org/10.4028/www.scientific.net/KEM.326-328.237.
[13] A.J. Schwartz, M. Kumar, B.L. Adams, D.P. Field, *Electron Backscatter Diffractionin in Materials Science* (Springer Science+Business Media, New York, 2009);
[14] D.J. Dingley, A.J. Wilkinson, G. Meaden, P.S. Karamched, *Elastic strain tensor measurement using electron backscatter diffraction in the SEM*, Journal of Electron Microscopy, 59(S1), S155 (2010); https://doi.org/10.1093/jmicro/dfq043.

[15] I. Fodchuk, S. Balovsyak, M. Borcha, Ya. Garabazhiv, V. Tkach, *Determination of structural inhomogeneity of synthesized diamonds by backscattering electron diffraction*, Physica Status Solidi A, 208(11), 2591 (2011); https://doi.org/10.1002/pssa.201184266.

[16] A. Wilkinson, B. Britton, *Strains, planes, and EBSD in materials science*, Materials Today, 15(9), 366 (2012); https://doi.org/10.1016/S1369-7021(12)70163-3.

[17] K. Hagihara, T. Okamoto, M. Yamasaki, Y. Kawamura, T. Nakano, *Electron backscatter diffraction pattern analysis of the deformation band formed in the Mg-based long-period stacking ordered phase*, Scripta Materialia, 117, 32 (2016); https://doi.org/10.1016/j.scriptamat.2016.02.016.

[18] A. Vilalta-Clemente, G. Naresh-Kumar, M. Nouf-Allehiani, P. Gamarra, M.A. di Forte-Poisson, C. Trager-Cowan, A.J. Wilkinson, *Cross-correlation based high resolution electron backscatter diffraction and electron channelling contrast imaging for strain mapping and dislocation distributions in InAlN thin films*, Acta Materialia, 125, 125 (2017); https://doi.org/10.1016/j.actamat.2016.11.039.

[19] T. B. Britton, J. L. R. Hickey, *Understanding deformation with high angular resolution electron backscatter diffraction (HR-EBSD)*, IOP Conference Series: Materials Science and Engineering 304, 012003 (2018); http://dx.doi.org/10.1088/1757-899X/304/1/012003.

[20] M.D. Borcha, S.V. Balovsyak, I.M. Fodchuk, V.Yu. Khomenko, V.N. Tkach, *Distribution of local deformations in diamond crystals according to the analysis of Kikuchi lines profile intensities*, Journal of Superhard Materials, 35(4), 220, (2013); https://doi.org/10.3103/S1063457613040035.

[21] I. Fodchuk, M. Solodkyi, M. Borcha, S. Balovsyak, V. Tkach, *Determination of local deformations and their anisotropy in polycrystalline Ge by electron backscatter diffraction data*, Metallofizika i Noveishie Tekhnologii, 41(3), 403 (2019); https://doi.org/10.15407/mfint.41.03.0403.

[22] M.D. Borcha, M.S. Solodkyi, S.V. Balovsyak, V.M. Tkach, I.I. Hutsuliak, A.R. Kuzmin, O.O. Tkach, V.P. Kladko, O.Yo. Gudymenko, O.I. Liubchenko, Z. Świątek, *Features of structural changes in mosaic Ge:Sb according to X-ray diffractometry and electron backscatter diffraction data*, Semiconductor Physics, Quantum Electronics and Optoelectronics, 22(4), 381 (2019); https://doi.org/10.15407/spqeo22.04.381.

[23] I. Fodchuk, S. Ivakhnenko, V. Tkach, S. Balovsyak, M. Borcha, N. Solodkii, I. Gutsulyak, A. Kuzmin, O. Sumaryuk, *Local strain distribution in synthetic diamond crystals, determined by the parameters of the energy spectrum of the Kikuchi patterns*, Journal of Superhard Materials, 42(1), 1 (2020); https://doi.org/10.3103/S1063457620010049.

[24] M.D. Borcha, M.S. Solodkyi, S.V. Balovsyak, I.M. Fodchuk, A.R. Kuzmin, V.M. Tkach, K.A. Yuschenko, A.V. Zviagintseva, *Determination of Local Strains in a Neighborhood of Cracks in a Welded Seam of Ni-Cr-Fe According to the Power Fourier Spectrum of Kikuchi Patterns*, Physics and Chemistry of Solid State, 19(4), 307 (2018); https://doi.org/10.15330/pcss.19.4.307-312.

[25] I. Fodchuk, S. Balovsyak, M. Borcha, Ya. Garabazhiv, V. Tkach, *Determination of Structural Homogeneity of Synthetic Diamonds With Analysis of Intensity Distribution of KikuchI Lines*, Semiconductor physics, quantum electronics and optoelectronics, 13(1), 262 (2010); https://doi.org/10.15407/spqeo13.03.262.

[26] M.D. Borcha, S.V. Balovsyak, I.M. Fodchuk, V.Yu. Khomenko, O.P. Kroitor, V.N. Tkach, *Local deformation in diamond crystals defined by the Fourier transformations of Kikuchi patterns*, Journal of Superhard Materials, 35(5), 284 (2013); https://doi.org/10.3103/S1063457613050031.

[27] M.D. Borcha, S.V. Balovsyak, I.M. Fodchuk, V.Yu. Khomenko, O.P. Kroitor, V.N. Tkach, *A strain state in synthetic diamond crystals by the data of electron backscatter diffraction method*, Journal of Superhard Materials, 38(4), 271 (2016); https://doi.org/10.3103/S1063457616040080.

[28] S. V. Balovsyak, O.V. Derevyanchuk, I. M. Fodchuk, *Method of calculation of averaged digital image profiles by envelopes as the conic sections*, Advances in Intelligent Systems and Computing, 754, 204 (2019); https://doi.org/10.1007/978-3-319-91008-6_21.

[29] S.V. Balovsyak, I.M. Fodchuk, *Objects Images Alignment with the Use of Genetic and Gradient Algorithms*, Komp'yutyng, 12(2), 160 (2013);

[30] F. Ram, S. Zaefferer, D. Raabe, *Kikuchi bandlet method for the accurate deconvolution and localization of Kikuchi bands in Kikuchi diffraction patterns*, Journal of Applied Crystallography, 47, 264 (2014); https://doi.org/10.1107/S1600576713030446.

[31] M. Borcha, I. Fodchuk, M. Solodkyi, S. Balovsyak, Yu. Roman, I. Hutsuliak, *Determination of structural heterogeneity of crystals from electron backscatter diffraction images with use of the Fourier energy spectrum*, Proc. SPIE, 11369, 113691I (2020); https://doi.org/10.1117/12.2553974.

[32] I. Fodchuk, S. Ivakhnenko, V. Tkach, S. Balovsyak, M. Solodkyi, M. Borcha, I. Hutsuliak, A. Kuzmin, Yu. Roman, Y. Smusenko, P. Pynuk, *Fourier energy analysis of Kikuchi patterns for investigation of defect system of diamond crystals*, Proc. SPIE, 12126, 121261M-6 (2021); https://doi.org/10.1117/12.2615864.

[33] I. Fodchuk, M. Solodkyi, S. Balovsyak, M. Borcha, I. Hutsuliak, M. Okolita, O. Tkach, *Local distribution of strains in synthetic diamond crystals determined by the energy spectrum normalized parameter*, Proc. SPIE, 12938, 129382F (2024); https://doi.org/10.1117/12.3015863.

[34] S. Thonhpanja, A. Phinyomark, P. Phukpattaranont, C. Limsakul, *Mean and Median Frequency of EMG Signal to Determine Muscle Force based on Time-dependent Power Spectrum*, Electronika IR Elektrotechnika, 19(3), 51 (2013); https://dx.doi.org/10.5755/j01.eee.19.3.3697.

[35] M. Borcha, I. Fodchuk, M. Solodkyi, M. Baidakova, *Structure diagnostics of heterostructures and multi-layered systems by X-ray multiple diffraction*, Journal of Applied Crystallography, 50(3), 722 (2017); https://doi.org/10.1107/S1600576717006574.

[36] I. Fodchuk, A. Kuzmin, I. Hutsuliak, M. Solodkyi, V. Dovganyuk, O. Maslyanchuk, Yu. Roman, R. Zaplitnyy, O. Gudymenko, V. Kladko, V. Molodkin, V. Lizunov, *Defect structure of high-resistivity CdTe:Cl crystals according to the data of high-resolution X-ray diffractometry*, Proceedings of SPIE, 11369, 113691H (2020); https://doi.org/10.1117/12.2553970.

І.М. Фодчук[1], С.В. Баловсяк[1], М.С. Солодкий[1], М.Д. Борча[1], Д.-І. Байле[2], Р. Лабудзький[3], М. Бонілла[4]

Просторові розподіли локальних деформацій в синтезованих кристалах алмазу із нормованих параметрів картин Кікучі

[1]*Чернівецький національний університет імені Юрія Федьковича, м. Чернівці, Україна, i.fodchuk@chnu.edu.ua*
[2]*Національний політехнічний університет науки і технологій Бухареста, Бухарест, Румунія*
[3]*Познанський технологічний університет, Познань, Польща*
[4]*Edibon International S.A., Мостолес, Іспанія*

У статті представлено вдосконалений підхід до розрахунку та аналізу просторових розподілів локальних деформацій в синтезованих кристалах алмазу, отриманих із нормованих параметрів картин Кікучі. Цей підхід полягає у вивченні картин Кікучі з використанням нормованих профілів смуг Кікучі та нормованих характеристик енергетичного спектру Фур'є дифракційних картин. Досліджено просторовий розподіл деформацій 6 зразків полікристалічного штучного алмазу. Проведено кластерний аналіз досліджуваних зразків кристалів, що дозволило встановити зв'язок між умовами росту кристалів алмазу та розподілом їх деформацій.

Ключові слова: штучний алмаз, дифракція зворотного розсіювання електронів, метод Кікучі, перетворення Фур'є, енергетичний спектр Фур'є, кластерний аналіз.